



Cite this: *Chem. Commun.*, 2016, 52, 6697

Received 16th February 2016,  
Accepted 18th April 2016

DOI: 10.1039/c6cc01433j

www.rsc.org/chemcomm

## A *de novo* self-assembling peptide hydrogel biosensor with covalently immobilised DNA-recognising motifs†

Patrick J. S. King,<sup>a</sup> Alberto Saiani,<sup>b</sup> Elena V. Bichenkova‡\*<sup>a</sup> and Aline F. Miller‡\*<sup>b</sup>

**We report here the first experimental evidence of a self-assembling three-dimensional (3D) peptide hydrogel, with recognition motifs immobilized on the surface of fibres capable of sequence-specific oligonucleotide detection. These systems have the potential to be further developed into diagnostic and prognostic tools in human pathophysiology.**

There has been a rapid development of new detection devices and biosensors over the past ten years, in particular, in the biomedical field where identification of single or multiple nucleotide polymorphisms could be crucial in recognising patient susceptibility to certain monogenic or complex diseases.<sup>1–6</sup> Modern DNA microarrays typically comprise of tens to thousands of 10–100 μm reaction sites, thus allowing the simultaneous analysis of thousands of nucleic acid sequences in a single experiment.<sup>7,8</sup> The majority of these systems rely on the sequence-specific hybridisation of target DNA or RNA sequences, with probe oligonucleotides immobilized to a surface, and typically use optical,<sup>9</sup> electrochemical<sup>10</sup> or gravimetric detection<sup>11</sup> to monitor binding events. There are still major challenges with such technology, which is limiting their successful transition to the commercial market.<sup>12–14</sup> These include high fabrication costs, poor sensitivity and accuracy, a lack of reproducibility, and significant divergence in the results of different devices on identical samples.<sup>15–17</sup> Moreover, even minor improvements in bioassay performance can very often be accompanied by substantial technological and conceptual complexity, which makes it incompatible with clinical application at point-of-care settings.<sup>18</sup> One approach to overcome such issues is to use a 3D polymer network as the solid-phase support. Such materials are relatively inexpensive, amenable to established detection techniques, and can enhance bioassay sensitivity due to a marked

increase in analyte storage capacity.<sup>19,20</sup> Their functionalization, however, is difficult to control and requires additional synthetic steps. Self-assembling peptide-based hydrogels share the desirable material properties, but in contrast their functionalization can be controlled precisely, on the molecular level using the principles of supramolecular chemistry.<sup>21</sup> Although they are currently more expensive to produce synthetically than simple polymers, there has been much recent progress towards reducing their cost significantly through bacterial expression.<sup>22</sup> Peptide hydrogels also benefit from providing a more biologically-relevant environment for sensing to occur,<sup>23</sup> ‘smart’ responsivity to stimuli such as pH and temperature,<sup>24–26</sup> self-healing properties that are amenable to rapid custom array production for personalised medicine, and can be dried for long-term storage, hence protecting oligonucleotides against nuclease degradation.<sup>27</sup> These biosensors are envisioned to be used in 96-well plates, or deposited onto chips, with analyte solution introduced onto the surface. Through the use of positively-charged hydrogels (+2 charge per peptide at pH 7, Fig. S1, see the ESI†), we aim to improve the biosensor sensitivity through an increase in the local concentration of negatively-charged target DNA around the sensing elements. The success of this approach has been previously reported in similar systems, such as in mercury detection using acrylamide gels.<sup>28</sup>

In this pilot study, the proof-of-principle level was achieved by using a simple molecular bio-recognition system which co-assembles with an octapeptide to form hydrogel-based biosensors capable of selectively hybridizing DNA and generating a fluorescence output (Fig. 1). This has never been reported before, and any previous attempts to incorporate DNA aptamers (*e.g. via* chemical modification during the gelation stage or *via* non-covalent attachment by mixing DNA aptamers within polymer gels) have not been successful due to the poor homogeneity, lack of reversibility, and undesirable leakage of DNA aptamers.<sup>29</sup>

The detection of the molecular DNA recognition and binding events was achieved here at the proof-of-principle level through hybridization between a DNA recognition motif CGATTCTGTGTT and a molecular beacon (MB) fluorescent probe F-5'-CGATTGCCA AACACAGAATCG-3'-D, where F is fluorescein and D is dabcyl. The

<sup>a</sup> Manchester School of Pharmacy, the University of Manchester, Stopford Building, Oxford Road, Manchester, M13 9PT, UK.  
E-mail: Elena.V.Bichenkova@manchester.ac.uk

<sup>b</sup> School of Chemical Engineering and Analytical Science, Manchester Institute of Biotechnology, 131 Princess Street, Manchester, M1 7DN, UK.  
E-mail: Aline.Miller@manchester.ac.uk

† Electronic supplementary information (ESI) available. See DOI: 10.1039/c6cc01433j

‡ These authors contributed equally to the work.



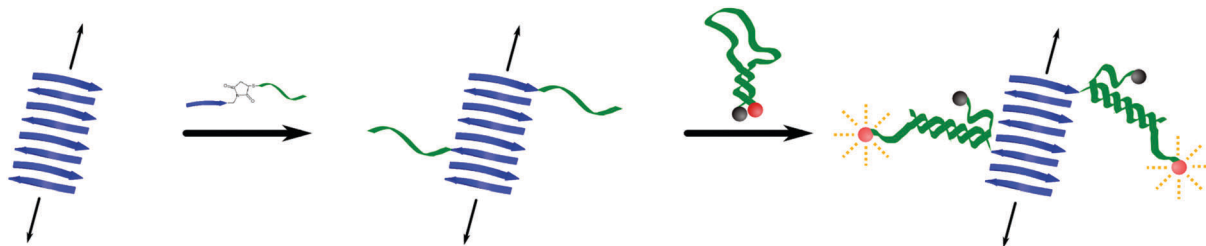


**Fig. 1** Design of a fluorescence-based peptide hydrogel DNA biosensor. (left) A self-assembling peptide hydrogel fibre comprising antiparallel  $\beta$ -sheets ( $\text{NH}_2$ -Val-Lys-Val-Lys-Val-Glu-Val-Lys-OH). (centre) Co-assembly of non-functionalised peptide and peptide-oligonucleotide conjugate immobilizes and displays oligonucleotide recognition motifs at the fibre surface. (right) MB probe hybridized with the tethered recognition sequence, causing the rapid development of strong fluorescence. Blue and green represent peptide and oligonucleotide, and red and black spheres represent fluorophore (fluorescein) and quencher (dabcyl), respectively.

recognition motif was conjugated to a modified version of the self-assembling peptide and incorporated into the peptide hydrogel through co-assembly with the base peptide (Fig. 1). In isolation, the MB forms an internal six-residue stem region that holds the fluorophore and quencher together to form a FRET pair (Fig. S2, see the ESI<sup>†</sup>), leading to a complete quenching of fluorescence. The stem region can be displaced by hybridization between the remaining single-stranded residues of the MB and the recognition motif, due to the formation of a more stable duplex comprising 12 Watson-Crick complementary base pairs. This leads to the separation of fluorescein and dabcyl and generates a strong fluorescence signal. The base peptide Val-Lys-Val-Lys-Val-Glu-Val-Lys was used in this pilot study as it is well-known to form flexible fibres comprising antiparallel  $\beta$ -sheets stacked perpendicular to their long axes (where Val is valine, Lys is lysine, and Glu is glutamic acid).<sup>30</sup> Above a critical concentration of 10 mM under physiological conditions these entangle to form hydrogels that contain >98% w/v water, with a swelling ratio of 51. The average fibre diameter was found to be 5.27 nm (SD = 0.54 nm,  $n = 50$ , Fig. S3, see the ESI<sup>†</sup>). Moreover, these short peptides have previously been shown to accommodate modified components within their structure, which are displayed and are accessible on the surface of the fibre.<sup>31–34</sup> No significant difference in fibre morphology was observed with the addition of analyte oligonucleotides or sensing elements (average diameter 5.02 nm, SD = 0.67 nm,  $n = 50$ , Fig. 3).

The peptide-oligonucleotide conjugate was synthesised by covalently linking the oligonucleotide CGATTCTGTGTT recognition sequence to the modified self-assembling peptide Gly-Gly-Val-Lys-Val-Lys-Val-Glu-Val-Lys using thiol-maleimide chemistry (Fig. S4, see the ESI<sup>†</sup>). The peptide was synthesised using standard Fmoc-based solid phase synthesis procedures and functionalized with *N*-maleoyl  $\beta$ -alanine at the *N*-terminus. The oligonucleotide was functionalised with a hexyl-thiol group at the 5' end. A two-glycine spacer was introduced to provide a flexible linker between the peptide fibres and the DNA recognition motif. The reaction was monitored using reversed-phase HPLC, and the isolated conjugate was characterised using <sup>1</sup>H NMR spectroscopy and mass spectrometry (Fig. S5 and S6, see the ESI<sup>†</sup>).

To validate the chosen system, hybridisation between the MB probe and its partner DNA was initially studied in solution (*i.e.* 100 mM TRIS buffer, pH 7.2, containing 200 mM KCl; full experimental details are given in the ESI<sup>†</sup>). In isolation, both

components (MB and unbound peptide-oligonucleotide conjugate) were entirely fluorescently silent (Fig. 2(A); blue and magenta curves, respectively), but when mixed together in an equimolar ratio in solution, a 100-fold (or greater) increase in MB fluorescence was observed at 518 nm ( $\lambda_{\text{ex}}$  494 nm, Fig. 2(A); black). This strong fluorescence signal is presumably due to hybridisation of the MB with the oligonucleotide component of the conjugate, causing the MB FRET pair to separate. The intensity of the generated fluorescence band (Fig. 2(A); black) was very similar to that produced by hybridisation of the MB with the free oligonucleotide CGATTCTGTGTT (Fig. 2(A); red), indicating that the binding ability of the oligonucleotide is largely unaffected by its conjugation to the peptide.

To determine whether the hydrogel environment had a detrimental effect on interactions between the MB and its partner, experiments identical to those described previously in TRIS buffer were performed, but within a hydrogel environment (21.5 mM base peptide, pH 7.2). As expected, the hydrogel was fluorescently silent (see Fig. 2(B); blue), while the MB

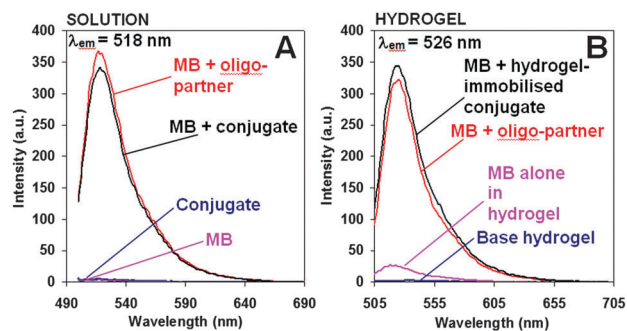


**Fig. 2** Fluorescence-based detection of hybridization. (A) Buffer solution: conjugate (blue) and MB (magenta) are fluorescently silent in isolation, but show a clear fluorescence response ( $\lambda_{\text{em}} = 518$  nm,  $\lambda_{\text{ex}} = 494$  nm) when mixed together (black), comparable with that observed for MB and oligonucleotide partner (red). (B) Hydrogel: the hydrogel is fluorescently silent (blue), while the MB shows some low background fluorescence in this environment (magenta). Hybridisation of the MB probe with the DNA-recognition motif incorporated into the 3D hydrogel generates a strong fluorescence signal (black;  $\lambda_{\text{em}} = 526$  nm,  $\lambda_{\text{ex}} = 494$  nm). This is higher than observed for MB and conjugate in a hydrogel environment (red). All components were at 1  $\mu\text{M}$  concentration for the experiments shown. Hydrogels formed using 21.5 mM peptide, at pH 7.



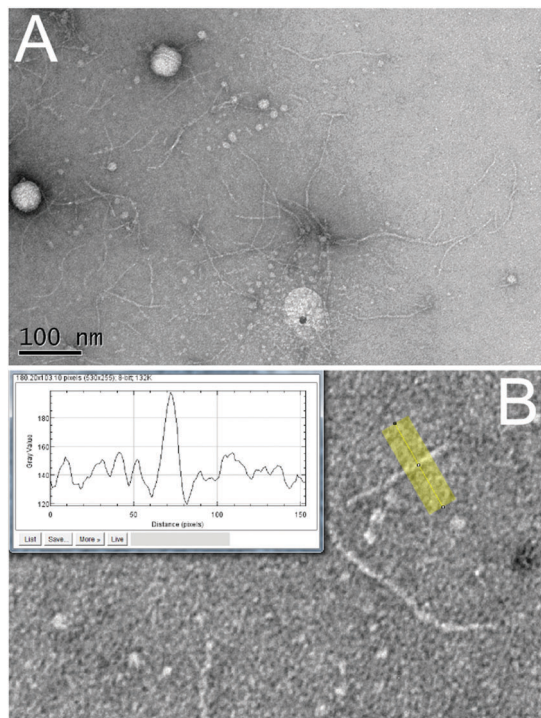


**Fig. 3** TEM images showing nanofibers that form Val-Lys-Val-Lys-Val-Glu-Val-Lys peptide hydrogels ( $20 \text{ mg ml}^{-1}$ , pH 7), co-assembled with  $1 \mu\text{M}$  peptide-oligonucleotide conjugate and  $1 \mu\text{M}$  partner to form the biosensor (A). Image analysis performed with ImageJ, using intensity profiles taken perpendicular to the fibre long axis (B). No significant difference in the fibre morphology was observed between blank hydrogels (Fig. S3, see the ESI<sup>†</sup>) and those with incorporated DNA-sensing components. The average fibre widths were  $5.27 \text{ nm}$  ( $\text{SD} = 0.54 \text{ nm}$ ,  $n = 50$ ) and  $5.02 \text{ nm}$  ( $\text{SD} = 0.67 \text{ nm}$ ,  $n = 50$ ), respectively. Full experimental details are given in the Materials and methods section.

showed some background fluorescence when physically mixed within the hydrogel (Fig. 2(B); magenta), presumably due to some degree of interaction between the MB and the hydrogel. The addition of the partner CGATTCTGTGTT to this system resulted in a 125-fold increase in the fluorescence as compared to the background fluorescence from the base hydrogel (Fig. 2(B); red). This showed a similar level of fluorescence enhancement as compared to that seen in the solution, demonstrating that the hydrogel did not have a detrimental effect on the hybridisation detection process. Interestingly, an 8 nm red-shift of the emission  $\lambda_{\text{max}}$  was observed, which presumably suggests that there is an interaction between the DNA and the oppositely-charged peptide fibres.

The performance of a self-assembling DNA hydrogel biosensor was directly compared with the analogous detection system in solution using identical concentrations of the MB and conjugate. To form the hydrogel-based biosensor, non-functionalised peptide ( $21.5 \text{ mM}$ , pH 7) was co-assembled with the peptide-oligonucleotide conjugate ( $1 \mu\text{M}$ ; giving a doping level of  $4.65 \times 10^{-3}\%$  within the hydrogel, Fig. 1). As such the oligonucleotide sequence should be exposed on the surface of the fibres, ready to hybridize with the complementary MB. As expected, the functionalised hydrogel remained fluorescently

silent over 24 hours of pre-incubation at  $20 \text{ }^\circ\text{C}$ . Gratifyingly, a strong fluorescence was immediately observed upon the addition of the MB (Fig. 2(B); black), with a similar intensity to that observed previously in homogeneous solutions (*i.e.* in TRIS buffer). The fluorescence emission of this fully-assembled model system was also red-shifted by 8 nm showing a fluorescence emission at  $\lambda_{\text{max}}$  at 526 nm. The rate of signal development was found to be approximately halved in a hydrogel environment compared with that in solution, as may be expected due to a slower rate of diffusion. The half-maximal signal was observed at 7.9 and 4.3 minutes after preparation, respectively (Fig. S7, see the ESI<sup>†</sup>).

To estimate the lowest limit of the conjugate doping level at which a detectable signal could still be confidently measured, an array of the hybridisation experiments were carried out (Fig. S8, see the ESI<sup>†</sup>), where the concentration of the peptide-oligonucleotide ranged from 200 to  $0.02 \text{ nM}$ . The base peptide concentration remained the same throughout the experiments at  $16.1 \text{ mM}$  to form weaker hydrogels, thus improving response times. The resulting doping level of the peptide-oligonucleotide conjugate relative to the non-functionalised peptide was varied, therefore, from  $1.24 \times 10^{-3}$  to  $1.24 \times 10^{-7}\%$ . To achieve this,  $250 \mu\text{l}$  of the hydrogel biosensor containing different doping levels of the peptide-oligonucleotide conjugate was deposited into individual wells in a 96-well plate, and incubated for 1 h at  $20 \text{ }^\circ\text{C}$ . The MB ( $50 \mu\text{l}$  aliquot) was introduced on top of hydrogel at molar concentrations identical to those of the DNA recognition components of the conjugate, and fluorescence spectra were recorded after 24 h of the incubation at  $20 \text{ }^\circ\text{C}$ . As can be seen from Fig. S8B (see the ESI<sup>†</sup>), the lowest concentration of the conjugate in the hydrogel that allowed detection with a reproducible signal (with the signal-to-noise ratio of 200:1) was  $50 \text{ pM}$ . This corresponds to a conjugate doping level of only  $3.11 \times 10^{-7}\%$ . The lowest concentration at which an immediate response can be observed was  $2 \text{ nM}$  ( $1.24 \times 10^{-5}\%$  doping, Fig. S8A, see the ESI<sup>†</sup>).

These experiments allowed us to explore the possibility of reducing the overall cost of bio-assay systems by considerably lowering the doping levels of the functionalised peptides within the hydrogel. Taking this further, we evaluated the analytical performance and capability of this novel biosensor by estimating the limit of detection (LoD) for this model assay system. This corresponded to the lowest quantity of the MB that can be reliably distinguished from the 'blank' sample, with a 95% confidence interval. The detection limit was estimated from the mean value of the 'blank' samples ( $n = 132$ ,  $\text{Mean}_{\text{blank}}$ ), the standard deviation of the 'blank' ( $\text{SD}_{\text{blank}}$ ) and the standard deviation of the 'low concentration sample' test replicates ( $n = 88$ ,  $\text{SD}_{\text{ics}}$ ) of a sample containing  $50 \text{ pM}$  analyte, using the published protocol.<sup>35</sup> Firstly, the limit of 'blank' (LoB) was estimated using eqn (1):

$$\text{LoB} = \text{Mean}_{\text{blank}} + 1.645(\text{SD}_{\text{blank}}) \quad (1)$$

Given a Gaussian distribution of the raw analytical signals from the 'blank' hydrogel samples, the LoB represents 95% of the



observed values, which corresponds to the 'zero' sample concentration. From this the LoD was estimated using eqn (2):<sup>35</sup>

$$\text{LoD} = \text{LoB} + 1.645(\text{SD}_{\text{ics}}) \quad (2)$$

The LoD was found to be 22 pM, which represents the lowest analyte concentration at which the detection is feasible using this pilot analytical system. This value is commensurate with other detection methods currently reported, demonstrating at the proof-of-principle level that a self-assembling peptide hydrogel can be used as the solid support on which molecular biorecognition oligonucleotide elements can be immobilized, to fish out and sense complementary DNA sequences. The strong fluorescence signal generated upon hybridisation provides the first experimental evidence of such a DNA-based biosensor that operates in 3D, and in a biologically-relevant environment.

In conclusion, we have demonstrated that *de novo* designed peptide-based hydrogels can be used as a 3D solid support on which oligonucleotides can be immobilized and be used to detect complementary sequences, with a detection limit of 22 pM. The lowest doping level of the conjugate in the hydrogel that allowed the detection of a reproducible fluorescence signal (with the signal-to-noise ratio of 200:1) was found to be  $3.11 \times 10^{-7}\%$ . This has not been accomplished before, and compares favourably with established 2D systems that use similar detection techniques. The unique properties of peptide hydrogels also enable the biomolecule detection under biologically-relevant conditions, minimize unwanted probe-probe interactions, and have the potential to hugely increase the analyte storage capacity of these devices. Here we have described a proof-of-concept system in which recognition elements are covalently attached to the hydrogel, and an MB sequence was used as a detector to signify the hybridisation event. Future work will focus on reversing the system, attaching the MB fluorescent probe to the peptide fibres to enable detection of unmodified, biologically-relevant sequences. Once accomplished, this technology has the potential to be applied towards the detection of other biomolecules, and even small molecules through the use of aptamers, which is of pressing need in areas such as drug identification, biomedical diagnostics, and pollutants in environmental monitoring.

The authors would like to thank the EPSRC National Mass Spectrometry Centre in Swansea for MS analysis of the peptidyl-oligonucleotide conjugate samples. PK also thanks the EPSRC (EP/H04986X/1) for financial support. AS thanks the EPSRC for financial support (EP/K016210/1). This work was also supported by the Wellcome Trust 'Research Consortia' Scheme [105610/Z/14/Z]. All research data supporting this publication are directly available within this publication.

## Notes and references

- 1 F. Payne, J. D. Cooper, N. M. Walker, A. C. Lam, L. J. Smink, S. Nutland, H. E. Stevens, J. Hutchings and J. A. Todd, *J. Leukocyte Biol.*, 2007, **81**, 581–583.
- 2 A. P. Chiang, J. S. Beck, H. J. Yen, M. K. Tayeh and T. E. Scheetz, *et al.*, *Proc. Natl. Acad. Sci. U. S. A.*, 2006, **103**, 6287–6292.
- 3 R. Kuwano, A. Miyashita, H. Arai, T. Asada and M. Imagawa, *Hum. Mol. Genet.*, 2006, **15**, 2170–2182.
- 4 Y. Takata, D. Hamada, K. Miyatake, S. Nakano, F. Shinomiya, C. R. Scafe, V. M. Reeve, D. Osabe, M. Moritani and K. Kunika, *Arthritis Rheum.*, 2007, **56**, 30–42.
- 5 M. A. Nouredine, X. J. Qin, S. A. Oliveira, T. J. Skelly and J. van der Walt, *Hum. Genet.*, 2005, **117**, 27–33.
- 6 E. Henke, J. Perk, J. Vider, P. Candia, Y. Chin, D. B. Solit, V. Ponomarev, L. Cartegni, K. Manova, N. Rosen and R. Benezra, *Nat. Biotechnol.*, 2008, **26**, 91–100.
- 7 J. Lamartine, *J. Mater. Sci. Eng.*, 2006, **26**, 354.
- 8 F. Bertucci, R. Houllatte, C. Nguyen, P. Viens, R. R. Jordan and D. Birnbaum, *Lancet Oncol.*, 2001, **2**, 674.
- 9 A. Charrier, N. Candoni, N. Liachenko and F. Thibaudan, *Biosens. Bioelectron.*, 2007, **22**, 1881–1886.
- 10 X. Yao, X. Li, F. Toledo, C. Zurita-Lopez, M. Gutova, J. Momand and F. Zhou, *Anal. Biochem.*, 2006, **354**, 220–228.
- 11 J. Pan, *Biochem. Eng. J.*, 2007, **35**, 183.
- 12 A. Mateescu, Y. Wang, J. Dostalek and U. Jonas, *Membranes*, 2012, **2**, 40–69.
- 13 J. Liu, *Soft Matter*, 2011, **7**, 6757–6767.
- 14 A. Sassolas, B. D. Leca-Bouvier and L. J. Blum, *Chem. Rev.*, 2008, **108**, 109–139.
- 15 S. Draghici, P. Khatri, A. C. Eklund and Z. Szallasi, *Trends Genet.*, 2006, **22**, 101–109.
- 16 A. Abdullah-Sayani, J. M. Bueno-de-Mesquita and M. J. Van de Vijver, *Nat. Clin. Pract. Oncol.*, 2006, **3**, 501–516.
- 17 P. K. Tan, T. J. Downey, E. L. Spitznagel, P. Xu, D. Fu, D. S. Dimitrov, R. A. Lempicki, B. M. Raaka and M. C. Cam, *Nucleic Acids Res.*, 2003, **31**, 5676–5684.
- 18 E. V. Bichenkova, Z. Lang, X. Yu, C. Rogert and K. T. Douglas, *Biochim. Biophys. Acta, Gene Regul. Mech.*, 2011, **1809**(1), 1–23; Y. Wang, A. Brunsen, U. Jonas, J. Dostalek and W. Knoll, *Anal. Chem.*, 2009, **81**, 9625–9632.
- 19 Y. Wang, A. Brunsen, U. Jonas, J. Dostalek and W. Knoll, *Anal. Chem.*, 2009, **81**, 9625–9632.
- 20 Y. Helwa, N. Dave, R. Froidevaux, A. Samadi and J. Liu, *ACS Appl. Mater. Interfaces*, 2012, **4**(4), 2228–2233.
- 21 H. Hosseinkhani, P. Hong and D. Yu, *Chem. Rev.*, 2013, **113**, 4837–4861.
- 22 C. Sonmez, K. J. Nagy and J. P. Schneider, *Biomaterials*, 2015, **37**, 62–72.
- 23 S. H. Gerhke, L. H. Uhden and J. F. McBride, *J. Controlled Release*, 1998, **55**, 21–33.
- 24 A. L. Boyle and D. N. Woolfson, *Chem. Soc. Rev.*, 2011, **40**, 4295–4306.
- 25 D. Chow, M. L. Nunalee, D. W. Lim, A. J. Simnick and A. Chilkoti, *Mater. Sci. Eng.*, 2008, **62**, 125–155.
- 26 X. P. Yang, X. H. Pan, J. Blyth and C. R. Lowe, *Biosens. Bioelectron.*, 2008, **23**, 899–905.
- 27 P. Dubruel, L. Dekie, B. Christiaens, B. Vanloo, M. Rosseneu, J. Vandekerckhove, M. Mannisto, A. Urtti and E. Schacht, *Biomacromolecules*, 2003, **4**, 1177–1183.
- 28 N. Dave, M. Y. Chan, P. J. Huang, B. D. Smith and J. Liu, *J. Am. Chem. Soc.*, 2010, **132**, 12668–12673.
- 29 M. Guvendiren, H. D. Lu and J. A. Burdick, *Soft Matter*, 2012, **8**, 260–272.
- 30 D. Roberts, C. Rochas, A. Saiani and A. F. Miller, *Langmuir*, 2012, **28**, 16196–16206.
- 31 C. Hickling, H. S. Toogood, A. Saiani, N. Scrutton and A. F. Miller, *Macromol. Rapid Commun.*, 2014, **35**, 868–874.
- 32 S. Piluso, H. C. Cassell, J. L. Gibbons, T. E. Waller, N. J. Plant, A. F. Miller and G. Cavalli, *Soft Matter*, 2013, **9**, 6752–6756.
- 33 A. Maslovskis, N. Tirelli, A. Saiani and A. F. Miller, *Soft Matter*, 2011, **7**, 6025–6033.
- 34 S. Boothroyd, A. Saiani and A. F. Miller, *Macromol. Symp.*, 2008, **273**, 139–145.
- 35 D. A. Armbruster and T. Pry, *Clin. Biochem. Rev.*, 2008, **29**(1), S49–S52.

